Transport in Porous Media **26:** 89–98, 1997.
© 1997 *Kluwer Academic Publishers. Printed in the Netherlands.*

Stokes Flow in a Slowly Varying Two-Dimensional Periodic Pore

PETER K. KITANIDIS* and BRUCE B. DYKAAR**
Stanford University, Stanford, CA 94305-4020, U.S.A.

(Received: 5 March 1996; in final form: 24 July 1996)

Abstract. This article presents a series solution to the velocity in a two-dimensional long sinusoidal channel. The approach is based on a stream function formulation of the Stokes problem and a series expansion in terms of the width to the length ratio, which is considered small. Results show how immobile zones may appear and even flow separation and nonturbulent eddies, even in the absence of *prima facie* dead-end pores. It is shown that the flow tends to concentrate in strips connecting pore throats.

Key words: Stokes flow, pore-scale hydrodynamics, analytical solution, multiple-scales method, stream function, biharmonic equation, periodic flow.

1. Introduction

Hydrogeologists and environmental engineers are typically interested in flow and transport at scales much larger than that of a single pore. For most applications, the smallest scale of interest is Darcy's scale where the pore structure is not resolved and the porous medium is regarded as a continuum. At that scale, flow is described through an equation based on Darcy's law and mass transport through the advection-dispersion-reaction equation; both equations are satisfied by bulk-averaged fluxes (e.g., Bear, 1972; Freeze and Cherry, 1979).

However, cognizance of flow and transport mechanisms at the pore scale is often essential in achieving a better grasp of phenomena observed at larger scales. A case in point is the presence of zones of immobile water which may impose mass transfer limitations and thus affect reaction rates, advective mass transport rates, and dispersive mixing (e.g., Dykaar and Kitanidis, 1996). There is considerable interest in understanding how immobile zones may be created and how flow may be reversed in 'dead end' pores and in fissures. The geometry of actual porous media is very complex and the solution of the Navier–Stokes equations or even the Stokes equations in so complicated flow domains is a formidable task. However, simplified geometries are useful in shedding light on processes (e.g., Edwards *et al.*, 1991) and in scaling up the equations to the Darcy scale (Brenner and Edwards, 1993). In most cases, numerical methods need to be employed (e.g., Pozrikidis, 1987; Edwards

* To whom all correspondence should be directed.
** Now at U.S. EPA, Corvallis, Oregon, U.S.A.

et al., 1991; Chen *et al.*, 1994). However, approximate analytical solutions have also been developed (e.g., Hasegawa and Izuchi, 1983) using a variety of methods.

In this work, we will compute Stokes flow in a long two-dimensional pore or fracture using a series approximation, which avoids the spatial discretization which is needed in the applications of finite differences, finite elements, and boundary elements. The method to be presented is similar to the perturbation approach of Hasegawa and Izuchi (1983) but differs from it in two respects:

- It follows a more systematic and rigorous rescaling method in order to formulate the sequence of equations that need to be solved to obtain sequentially terms in the series.
- It uses an auxiliary condition based on an energy argument, that is physically intuitive and precise, unlike the reasonable but *ad hoc* auxiliary condition used by Hasegawa and Izuchi (1983).

2. Problem Formulation

We consider a channel that is two-dimensional and symmetric about the straight axis. The width of the channel is a smooth periodic function, such as

$$w(x) = \bar{w} + 2a \sin\left(2\pi \frac{x}{L}\right) \tag{1}$$

and the half-width is

$$h(x) = \frac{\bar{w}}{2} + a \sin\left(2\pi \frac{x}{L}\right), \tag{2}$$

where $\bar{w}$ is the average width and $\bar{w} + 2a$ is the maximum width, $a < \bar{w}/2$. The fluid is incompressible and the flow is steady and periodic.

The governing equations are incompressibility and Stokes equations

$$\frac{\partial u}{\partial x} + \frac{\partial v}{\partial y} = 0, \tag{3}$$

$$\frac{\partial p}{\partial x} = \mu \left(\frac{\partial^2 u}{\partial x^2} + \frac{\partial^2 u}{\partial y^2}\right), \tag{4}$$

$$\frac{\partial p}{\partial y} = \mu \left(\frac{\partial^2 v}{\partial x^2} + \frac{\partial^2 v}{\partial y^2}\right), \tag{5}$$

where u and v are flow velocities in the direction of flow x and y, respectively; p is the dynamic pressure, which is related to the hydraulic head ϕ through $p = \rho g \phi$; and μ is the viscosity coefficient. As is well known, the Stokes equations are obtained from the Navier–Stokes equations when the flow is slow, i.e. the Reynolds number is small. This condition is met in most flows in porous media. Excellent

references on the subject are Happel and Brenner (1983), who also provide a historical perspective, and Pozrikidis (1992).

Introduce the stream function

$$u = \frac{\partial \Psi}{\partial y}, \qquad v = -\frac{\partial \Psi}{\partial x}. \tag{6}$$

Inserting in the governing equations and after elimination of the pressure term, we find that the stream function satisfies the biharmonic equation (*ibid.*):

$$\nabla^4 \Psi = \frac{\partial^4 \Psi}{\partial x^4} + 2\frac{\partial^4 \Psi}{\partial x^2 \partial^2 y} + \frac{\partial^4 \Psi}{\partial y^4} = 0. \tag{7}$$

Mathematically, the problem is reduced to solving the biharmonic.

Boundary conditions include the no-flux and no-slip conditions on the solid boundary. In search of additional auxiliary conditions, we will make use of the periodicity.

$$p(x + L, y) = p(x, y) + \Delta p, \tag{8}$$

$$\begin{aligned} &u(x + L, y) = u(x, y), \qquad v(x + L, y) = v(x, y), \\ &\Psi(x + L, y) = \Psi(x, y), \end{aligned} \tag{9}$$

where the drop per period is $\Delta p < 0$. Application of the energy equation within a periodic cell yields

$$\int_V 2\mu\Theta \, \mathrm{d}V = -\Delta p Q, \tag{10}$$

where

$$\begin{aligned} \Theta &= \left(\frac{\partial u}{\partial x}\right)^2 + \frac{1}{2}\left(\frac{\partial u}{\partial y} + \frac{\partial v}{\partial x}\right)^2 + \left(\frac{\partial v}{\partial y}\right)^2 \\ &= \left(\frac{\partial^2 \Psi}{\partial x \partial y}\right)^2 + \frac{1}{2}\left(\frac{\partial^2 \Psi}{\partial y^2} - \frac{\partial^2 \Psi}{\partial x^2}\right)^2 + \left(\frac{\partial^2 \Psi}{\partial y \partial x}\right)^2. \end{aligned} \tag{11}$$

The meaning of Equation (10) is that the viscous dissipation within the unit cell, is equal to the work done by surface forces on the control volume (e.g., Kundu, 1990). Equation (10) is the auxiliary condition that we will use later. Application of (10) is a key difference form previous work (Hasegawa and Izuchi, 1983) which used an *ad hoc* condition.

Also, for future reference, we will define $\bar{Q}$ as the discharge that would take place in a channel with uniform width $\bar{w}$

$$\bar{Q} = -\frac{\bar{w}^3}{12\mu}\frac{\Delta p}{L}. \tag{12}$$

This cubic law is the result of the classic plane Poiseuille flow problem of fluid mechanics (Happel and Brenner, 1983, p. 34). Regarding the use of the cubic law for flow through single fractures, see Gale *et al.* (1985), Hull *et al.* (1987), Raven, *et al.* (1988).

An exact analytic solution is probably impossible to obtain but approximations can be obtained for a long channel in a series in terms of the small dimensionless parameter

$$\epsilon = \frac{\bar{w}}{L}. \tag{13}$$

The idea is to take advantage of the fact that variation in the direction of flow x is slow compared to variation in the orthogonal direction y.

3. Nondimensionalization

First, we make all distances dimensionless by dividing all lengths by $\bar{w}$. (This is equivalent to selecting as unit length $\bar{w}$.) We make discharge and stream-function values dimensionless by dividing them by $\bar{Q}$. To keep the notation simple, we will use the same symbols for the dimensionless variables, except that $\bar{w}$ is replaced by 1. Just keep in mind that after this point, all variables are dimensionless.

With nondimensional variables, the governing equation has the same form (7) and the auxiliary condition becomes:

$$\frac{1}{6L}\int_0^L \int_{-h}^{h} \Theta \, \mathrm{d}x \, \mathrm{d}y = Q. \tag{14}$$

4. Rescaling

Note that x varies from 0 to L and y varies from $-h$ to h. The next crucial step is to introduce the rescaled variables (e.g., Hinch, 1991)

$$\eta = \frac{x}{L} = \epsilon x, \qquad \xi = \frac{y}{h(\eta)} = \frac{y}{h(\epsilon x)} \tag{15}$$

(note that ϵ is indeed equal to the ratio $\bar{w}/L$), where

$$h(\eta) = \tfrac{1}{2} + a \sin(2\pi\eta) \tag{16}$$

and we seek the stream function in terms of the rescaled variables, i.e., we seek $\Psi(\eta, \xi)$.

$$\Psi = \Psi_0 + \epsilon\Psi_1 + \epsilon^2\Psi_2 + \cdots, \tag{17}$$

where Ψ_i are functions of η and ξ to be found. Applying to Equation (7) and auxiliary conditions and separating terms of the same order of ϵ, we will obtain a sequence of boundary-value problems.

The auxiliary condition using the rescaled variables is

$$\frac{1}{6}\int_0^1\int_{-1}^1 h(\eta)\Theta\,\mathrm{d}\xi\,\mathrm{d}\eta = Q. \tag{18}$$

5. Zero-Order Terms

Keeping terms of zero order in (7)

$$\frac{\partial^4\Psi_0}{\partial\xi^4} = 0, \tag{19}$$

$$\Psi_0 = C_0 + C_1\xi + C_2\xi^2 + C_3\xi^3. \tag{20}$$

The no slip boundary conditions are $\partial\Psi_0/\partial\xi = 0$ at $\xi = \pm 1$. We also specify that total flux is Q_0, to be found later, so that $\Psi_0 = -Q_0/2$ at $\xi = -\frac{1}{2}$ and $\Psi_0 = Q_0/2$ at $\xi = \frac{1}{2}$. Thus

$$\Psi_0 = Q_0(\tfrac{3}{4}\xi - \tfrac{1}{4}\xi^3). \tag{21}$$

We then use the auxiliary condition (10) keeping terms of zero order:

$$\Theta = \frac{1}{2}\left(\frac{\partial^2\Psi_0}{\partial y^2}\right)^2 = \frac{1}{2h^4}\left(-\frac{3}{2}Q_0\xi\right)^2 = \frac{9}{8h^4}Q_0^2\xi^2,$$

$$Q = Q_0,$$

where $h = h(\eta)$. Thus (10) becomes

$$\frac{Q_0}{8}\int_0^1 \frac{1}{h^3}\,\mathrm{d}\eta = 1, \tag{22}$$

or

$$Q_0 = 8\left[\int_0^1 \frac{1}{h^3}\,\mathrm{d}\eta\right]^{-1} = \left[\int_0^1 \frac{1}{w^3}\,\mathrm{d}\eta\right]^{-1}.$$

This zero-order solution already captures many important characteristics. The streamlines adjust to the wavy wall, consistent with the results of numerical models (Pozrikidis, 1987). The solution also clearly demonstrates that the sinuosity of the channel lowers the discharge*, *ceteris paribus*. The reason is that the increase

* Note that in dimensional terms, the discharge is

$$Q_0 = \bar{Q}\left[\int_0^1 \frac{1}{w^3(\eta)}\,\mathrm{d}\eta\right]^{-1} = -\frac{\bar{w}^3}{12\mu}\frac{\Delta p}{L}\left[\int_0^1 \frac{1}{w^3(\eta)}\,\mathrm{d}\eta\right]^{-1}.$$

in viscous dissipation near channel throats is much larger than the decrease in channel hollows. It is worth noting that the zero-order solution is essentially the same approximation used in the well known 'lubrication theory' (Zimmerman *et al.*, 1991, review the applicability of this approach to flow in fractures). However, this approximation does not capture the possibility of flow reversal in wall cavities, a phenomenon that has been observed in numerical and experimental studies.

6. Second-Order Terms

The first-order terms vanish and we proceed to the second-order terms. The biharmonic reduces to:

$$2\left[(6h_\eta^2 - 2hh_{\eta\eta})\frac{\partial^2\Psi_0}{\partial\xi^2} + (6h_\eta^2 - hh_{\eta\eta})\xi\frac{\partial^3\Psi_0}{\partial\xi^3}\right] + \frac{\partial^4\Psi_2}{\partial\xi^4} = 0, \tag{23}$$

where $h = h(\eta)$, $h_\eta = \frac{\partial h}{\partial\eta}$, and $h_{\eta\eta} = \frac{\partial^2 h}{\partial\eta^2}$.

Using

$$\frac{\partial^2\Psi_0}{\partial\xi^2} = -\tfrac{3}{2}Q_0\xi, \qquad \frac{\partial^3\Psi_0}{\partial\xi^3} = -\tfrac{3}{2}Q_0, \tag{24}$$

$$-3[(6h_\eta^2 - 2hh_{\eta\eta}) + (6h_\eta^2 - hh_{\eta\eta})]Q_0\xi + \frac{\partial^4\Psi_2}{\partial\xi^4} = 0, \tag{25}$$

or, after simplifications

$$-A\xi + \frac{\partial^4\Psi_2}{\partial\xi^4} = 0, \qquad A = 9(4h_\eta^2 - hh_{\eta\eta})Q_0. \tag{26}$$

Integrating the differential equation

$$\Psi_2(\xi) = \tfrac{1}{120}A\xi^5 + C_1 + C_2\xi + C_3\xi^2 + C_4\xi^3. \tag{27}$$

The boundary conditions are: no-slip $\partial\Psi_2/\partial\xi = 0$ at $\xi = \pm 1$; $\Psi_2 = -Q_2/2$ at $\xi = -\frac{1}{2}$ and $\Psi_2 = Q_2/2$ at $\xi = \frac{1}{2}$, where Q_2 is to be found later.

$$\begin{aligned}
&\tfrac{1}{24}A + C_2 - 2C_3 + 3C_4 = 0,\\
&\tfrac{1}{24}A + C_2 + 2C_3 + 3C_4 = 0,\\
&-\tfrac{1}{120}A + C_1 - C_2 + C_3 - C_4 = -\frac{Q_2}{2},\\
&\tfrac{1}{120}A + C_1 + C_2 + C_3 + C_4 = \frac{Q_2}{2}.
\end{aligned}$$

Solution is $\{C_3 = 0, C_1 = 0, C_4 = -\frac{1}{60}A - \frac{1}{4}Q_2, C_2 = \frac{1}{120}A + \frac{3}{4}Q_2\}$. Substituting

$$\begin{aligned}
&\Psi_2(\xi) = \tfrac{1}{120}A\xi^5 + (\tfrac{1}{120}A + \tfrac{3}{4}Q_2)\xi - (\tfrac{1}{60}A + \tfrac{1}{4}Q_2)\xi^3,\\
&\Psi_2 = \tfrac{1}{120}A(\xi^5 - 2\xi^3 + \xi) + \tfrac{1}{4}Q_2(3\xi - \xi^3).
\end{aligned} \tag{28}$$

Equating the second-order terms in the auxiliary condition, we obtain

$$Q_0 \int_0^1 \frac{5Q_2 + 5Q_0 h_\eta^2 - Q_0 h h_{\eta\eta}}{20h^3}\,\mathrm{d}\eta = Q_2. \tag{29}$$

After simplifications,

$$Q_2 = \frac{Q_0^2}{20} \int_0^1 \frac{h h_{\eta\eta} - 5h_\eta^2}{h^3}\,\mathrm{d}\eta. \tag{30}$$

7. Fourth-Order Terms

Following the same procedure as in the previous two cases, we obtain the solution:

$$\begin{aligned}\Psi_4 \;=\; & Q_4(\tfrac{3}{4}\xi - \tfrac{1}{4}\xi^3) - Q_2 \tfrac{3}{40}(h h_{\eta\eta} - 4h_\eta^2)\xi(1-\xi^2)^2 - \\ & - \frac{Q_0}{5600}((408 + 1800\xi^2)h_\eta^4 + (684 - 1800\xi^2)h h_\eta^2 h_{\eta\eta} - \\ & - (270 - 180\xi^2)h^2 h_{\eta\eta}^2 - (248 - 240\xi^2)h^2 h_\eta h_{\eta\eta\eta} + \\ & + (19 - 15\xi^2)h^3 h_{\eta\eta\eta\eta})\xi(1-\xi^2)^2.\end{aligned}$$

Then, the auxiliary condition is used to compute the fourth-order discharge term Q_4.

$$\begin{aligned}&\frac{175}{1400}Q_2^2\frac{8}{Q_0} + \frac{350}{1400}Q_4 Q_0 \frac{8}{Q_0} + \frac{1}{1400}Q_0 Q_2 \int_0^1 \frac{700h_\eta^2 - 140 h h_{\eta\eta}}{h^3}\,\mathrm{d}\eta + \\ &\quad + \frac{Q_0^2}{1400}\int_0^1 \frac{87h_\eta^4 - 306 h h_\eta^2 h_{\eta\eta} + 54h^2 h_{\eta\eta}^2 + 56h^2 h_\eta h_{\eta\eta\eta} - 4h^3 h_{\eta\eta\eta\eta}}{h^3}\,\mathrm{d}\eta.\end{aligned} \tag{31}$$

Simplifying

$$\begin{aligned}Q_4 \;=\; & \frac{Q_2^2}{Q_0} - \frac{Q_0^2}{1400} \times \\ & \times \int_0^1 \frac{87h_\eta^4 - 306 h h_\eta^2 h_{\eta\eta} + 54h^2 h_{\eta\eta}^2 + 56h^2 h_\eta h_{\eta\eta\eta} - 4h^3 h_{\eta\eta\eta\eta}}{h^3}\,\mathrm{d}\eta.\end{aligned} \tag{32}$$

8. Summary

Compute the integrals

$$Q_0 = 8\left[\int_0^1 \frac{1}{h^3}\,\mathrm{d}\eta\right]^{-1}, \tag{33}$$

$$Q_2 = \frac{Q_0^2}{20} \int_0^1 \frac{hh_{\eta\eta} - 5h_\eta^2}{h^3}\, \mathrm{d}\eta, \tag{34}$$

$$\begin{aligned} Q_4 \;=\; & \frac{Q_2^2}{Q_0} - \frac{Q_0^2}{1400} \times \\ & \times \int_0^1 \frac{87h_\eta^4 - 306hh_\eta^2 h_{\eta\eta} + 54h^2 h_{\eta\eta}^2 + 56h^2 h_\eta h_{\eta\eta\eta} - 4h^3 h_{\eta\eta\eta\eta}}{h^3}\, \mathrm{d}\eta \end{aligned} \tag{35}$$

and the total flux is

$$Q \simeq Q_0 + \epsilon^2 Q_2 + \epsilon^4 Q_4.$$

The stream functions are

$$\Psi_0 = Q_0(\tfrac{3}{4}\xi - \tfrac{1}{4}\xi^3), \tag{36}$$

$$\Psi_2(\xi) = \frac{3Q_0}{40}[4h_\eta^2 - hh_{\eta\eta}](\xi^5 - 2\xi^3 + \xi) + Q_2(\tfrac{3}{4}\xi - \tfrac{1}{4}\xi^3), \tag{37}$$

$$\begin{aligned} \Psi_4 \;=\; & Q_4(\tfrac{3}{4}\xi - \tfrac{1}{4}\xi^3) - Q_2 \tfrac{3}{40}(hh_{\eta\eta} - 4h_\eta^2)\xi(1-\xi^2)^2 - \\ & - \frac{Q_0}{5600}((408 + 1800\xi^2)h_\eta^4 + (684 - 1800\xi^2)hh_\eta^2 h_{\eta\eta} - \\ & - (270 - 180\xi^2)h^2 h_{\eta\eta}^2 - (248 - 240\xi^2)h^2 h_\eta h_{\eta\eta\eta} + \\ & + (19 - 15\xi^2)h^3 h_{\eta\eta\eta\eta})\xi(1-\xi^2)^2, \end{aligned}$$

$$\Psi \simeq \Psi_0 + \epsilon^2 \Psi_2 + \epsilon^4 \Psi_4. \tag{38}$$

9. Results

Consider, first, the case that the normalized amplitude is $a/\bar{w} = 0.4$ and the normalized length is $L/\bar{w} = 5$. The stream lines are shown in Figure 1 with solid lines delineating stream tubes that convey $\frac{1}{8}$ of total flow. For added resolution near the wall, dotted lines delineate stream tubes with $\frac{1}{40}$ of the flow. The average velocity in each tube being inversely proportional to the width of the tube, it is clear from this figure that the flow in a sizeable region near the wall in the hollow part of the pore is much lower than the mean flow velocity. Advective transport and mixing in this region is low. At the throat (narrow part) of the pore, it is worth noting that the flow is shooting through at a high velocity near the center of the channel.

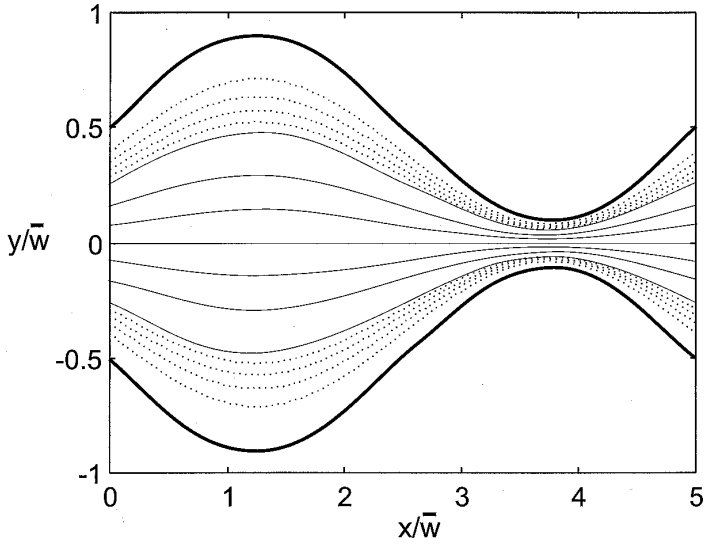

Figure 1. Stream lines for $a/\bar{w} = 0.4$ and $l/\bar{w} = 5$.

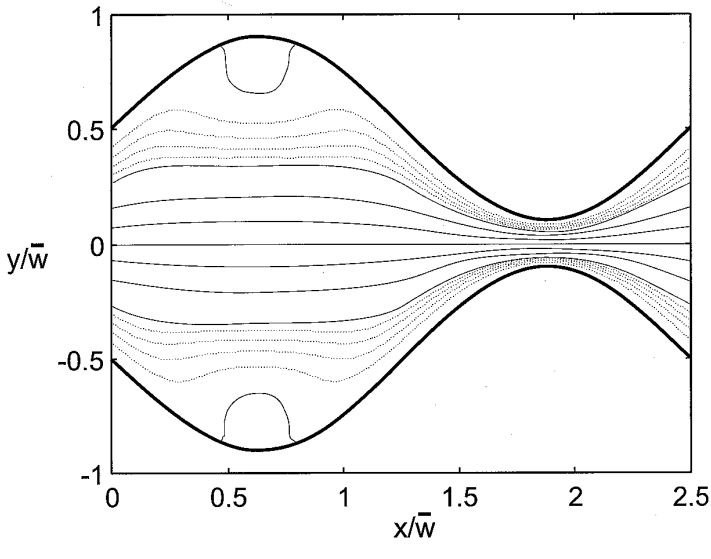

Figure 2. Stream lines for $a/\bar{w} = 0.4$ and $l/\bar{w} = 2.5$.

As the length to width ratio decreases, the immobile zone grows in size. At some value, stagnation points appear on the well and flow separation occurs. Consider, for example, $a/\bar{w} = 0.4$ and $L/\bar{w} = 2.5$. As the stream lines depicted in Figure 2 demonstrate, most of the flow takes place within a canal from one pore throat to the next. In the rest of the pore space the water flows much more slowly, forming what is practically an immobile zone, despite the fact that the pore does not appear

as ‘dead end’. The vortices indicated in Figure 2 by the closed streamlines are nonturbulent: the form of each vortex depends only on the pore geometry and the velocity is proportional to the average flow velocity. Although the velocity in the eddies is much smaller than the mean velocity, these eddies may increase the mixing in the immobile zone and enhance the effective reaction rate in diffusion limited heterogeneous reactions, such as in the case of biofilms (Dykaar and Kitanidis, 1996).

Acknowledgements

Funding from this study was provided by the office of Research and Development, U.S. EPA, under agreement R-819751-01 through the Western Region Hazardous Substance Research Center and by the National Science Foundation under project EAR-9523922, ‘Constitutive Relations of Solute Transport and Transformation’.

References

Bear, J.: 1972, *Dynamics of Fluids in Porous Media*, American Elsevier, New York.

Brenner, H., and Edwards, D. A.: 1993, *Macrotransport Processes*, Butterworth-Heinemann, Boston.

Chen, B., Cunningham, A., Ewing, R., Peralta, R. and Visser, E.: 1994, Two-dimensional modeling of microscale transport and biotransformation in porous media, *Numer. Methods Partial Differential Equations* **10**, 65–83.

Hasegawa, E. and Izuchi, H.: 1983, On steady flow through a channel consisting of an uneven wall and a plane wall. Part 1. Case of no relative motion in two walls, *Bull. JSME* **26**(214), 514–520.

Dykaar, B. B.: 1994, Macroflow and macrotransport in heterogeneous porous media, PhD Thesis, Stanford Univ. Civ. Eng.

Dykaar, B. B. and Kitanidis, P. K.: 1996, Macrotransport of a biologically reacting solute through porous media, *Water Resour. Res.* **32**(2), 307–320.

Edwards, D.A., Shapiro, M., Bar-Yoseph, P. and Shapira, M.: 1990, The influence of Reynolds number upon the apparent permeability of spatially periodic arrays of cylinders, *Phys. Fluids A* **2**(1), 45–55.

Edwards, R. A., Shapiro, M., Brenner, H. and Shapira, M.: 1991, Dispersion of inert solute in spatially periodic two-dimensional model porous media, *Transport in Porous Media* **6**, 337–358.

Freeze, R. A. and Cherry, J. A.: 1979, *Groundwater*, Prentice-Hall, New York.

Gale, J. E., Rouleau, A. and Atkinson, L. C.: 1985, Hydraulic properties of fractures, in *Memoires. Hydrogeology of Rocks of Low Permeability*, International Association of Hydrogeologists, Tucson, AZ, pp. 1-11.

Happel, J. and Brenner, H.: 1983, *Low-Reynolds Number Hydrodynamics*, Kluwer, Boston.

Hinch, E. J.: 1991, *Perturbation Methods*, Cambridge Univ. Press, Cambridge.

Hull, L. C., Miller, J. D. and Clemo, T. M.: 1987, Laboratory and simulation studies of solute transport in fracture networks, *Water Resour. Res.* **23**(8), 1505–1513.

Kundu, P. K.: 1990, *Fluid Mechanics*, Academic Press, San Diego.

Pozrikidis, C.: 1987, Creeping flow in two-dimensional channels, *J. Fluid Mech.* **180**, 495–514.

Pozrikidis, C.: 1992, *Boundary Integral and Singularity Methods for Linearized Viscous Flow*, Cambridge Univ. Press.

Raven, K. G., Novakowski, K. S. and Lapcevic, P. A.: 1998, Interpretation of field tracer tests of a single fracture using a transient solute storage model, *Water Resour. Res.* **24**(12), 2019–2032.

Zimmerman, R. W., Kumar, S. and Bodvarsson, G. S.: 1991, Lubrication theory analysis of the permeability of rough-walled fractures, *Int. J. Rock Mech. Min. Sci. Geomech. Abstr.* **28**(4), 325–331.